Multimed Tools Appl (2016) 75:1079–1098
DOI 10.1007/s11042-014-2358-7

A new strategy of image denoising using multiplier-less FIR filter designed with the aid of differential evolution algorithm

Abhijit Chandra · Sudipta Chattopadhyay

Received: 23 November 2013 / Revised: 15 September 2014 / Accepted: 7 November 2014 /
Published online: 20 November 2014

Abstract Due to the rapid development of one-dimensional signal processing in last few decades, it has spread out its wings in the field of multi-dimensional signal processing too. This has mainly been dominated by the proposition and implementation of robust algorithms which have focused on efficient storage and reliable transmission of digital images of various kinds. During the transmission through wired or wireless medium, digital images often encountered different types of channel noise which can significantly distort its appearance. As a matter of fact, filtering operation of digital images forms one of the most important tasks to be performed at the receiving end. In this paper, we have proposed a novel design strategy of two-dimensional (2-D) low-pass filter by means of a powerful evolutionary optimization technique called Differential Evolution (DE) algorithm. Mask coefficients of the proposed filter are constrained to assume values as sum of powers-of-two, thus making the filter hardware friendly. Experimental results have demonstrated the power of the algorithm in reducing the effect of Gaussian noise from digital image in terms of various performance parameters like peak signal-to-noise ratio (PSNR), structural similarity index measure (SSIM), image enhancement factor (IEF) and image quality index (IQI) and so on. A number of test images have been taken into our consideration for the purpose of establishing our proposition. Simulation results have confirmed the superiority of the proposed DE-based filter over the conventional low-pass filtering method.

Keywords Differential Evolution (DE) algorithm · Image enhancement factor (IEF) · Image quality index (IQI) · Gaussian noise · Multiplier-less low-pass filter · Peak signal-to-noise ratio (PSNR) · Structural similarity index measure (SSIM)

A. Chandra (✉)
Department of Instrumentation & Electronics Engineering, Jadavpur University, Sector III, Block LB, Plot No. 8 Salt Lake Bypass, Salt Lake City, Kolkata 700 098, India
e-mail: abhijit922@yahoo.co.in

S. Chattopadhyay
Department of Electronics & Telecommunication Engineering, Jadavpur University, Kolkata 700 032, India
e-mail: sudiptachat@yahoo.com

1 Introduction

Design of 2-D digital filter has grown sufficient interest amongst the researchers over the last few decades. A number of well developed algorithms are available in the literature nurturing the concept of image filter design and these include methods like windowing, frequency sampling, linear programming, Chebyshev technique and so on [14]. Although these techniques can produce filters which can closely approximate ideal response, they are often challenged because of their computationally ineffective method of implementation especially for higher order filters. In connection to this, design of a 2-D linear phase FIR filter has been facilitated from a 1-D linear phase FIR filter which can give rise to high computational efficiency. Three simple and efficient transformations based on original McClellan transformation for the design of 2-D FIR filters have been recently proposed in [13]. Besides producing circularly symmetric wideband and multiple-band 2-D filters, it is equally suitable for narrowband applications.

A number of approaches had been taken in practice towards the realization of 2-D FIR filter by means of evolutionary optimization techniques of current interest and the supremacy of such design over equivalent filters designed with the aid of linear programming and simulated annealing has been firmly established [16]. An effective genetic algorithm (GA) approach has been recently proposed in [22] for designing two-dimensional FIR digital filter with prescribed magnitude and phase responses. By minimizing a quadratic measure of error in the frequency band, the real-valued chromosomes of a population are evolved to get the filter coefficients. Author has demonstrated the efficiency of the algorithm by listing two design examples. Design of both linear shift-invariant (LSIV) and periodically shift-variant (PSV) 2-D separable denominator filters with single powers-of-two coefficients has been achieved with the aid of binary-GA and integer-GA in [20] and [19]. Use of the second approach reduces the chromosome size and hence makes the algorithm much faster. On the other hand, binary-GA tends to get closer to the solution and thereby yields lower cost function. An optimal design method of 2-D FIR filter based on GAs has been introduced in [2] whose key point stems in the capacity to adapt the genetic operators during the genetic life while remaining simple and easy to implement. Authors have claimed that their adaptive GA-based approach can produce filters with good response characteristics in minimum CPU time. The notion of artificial intelligence has enriched the other relevant applications of image processing like digital watermarking [9–11], pattern recognition [25] as well.

Incorporation of evolutionary algorithms like GA has made silent revolution in the field of scientific research by virtue of the fact that they can be employed to search for optimum solution over rough, discontinuous and multi-modal surface which cannot be easily optimized by any conventional methods. However, GA suffers from the tendency of premature convergence, exponentially increasing computation time with increasing population size and even its average fitness can become worse [3]. In regard to this, DE has opened a new door which can eliminate the shortcomings of GA by producing results with higher convergence speed and better accuracy [17, 18]. Robustness of DE in optimizing the mask coefficients of multiplierless 2D filter has therefore been judiciously employed in this work.

Reduction of noise from the digital image has been carried out through several means which can be broadly classified into two categories, namely linear and non-linear spatial filtering and transform domain filtering. These approaches basically filter out the high frequency noise from the image and may cause unwanted smoothing of the image details like edge, corner etc. Several researchers have proposed different methodologies on image denoising like bilateral filtering (BF) [21], stochastic denoising (SD) [6] and so on. Recently a denoising method has been proposed through 2-D FIR filtering approach in [8] where the coefficients are generated by the Differential Evolution Particle Swarm Optimization (DEPSO) algorithm. By means of computer simulation, it has been demonstrated that the proposed method is superior to conventional low-pass filtering method like mean, median filter as well as the modern BF and SD method. An efficient decision-based, couple window-based median filtering algorithm for the restoration of high density salt-and-pepper noise corrupted image has been recently proposed in [1] which had been constructed as a combination of noisy pixel detection stage followed by a filtering stage. Apart from removing the high density salt-and-pepper noise, proposed algorithm also preserves the fine details of four different images considered in the article.

In this paper, we have proposed a novel idea of 2-D multiplier-less low-pass FIR filter design with the aid of a robust optimization technique, called Differential Evolution (DE) algorithm. Mask coefficients of the designed filter have been selected from a set of finite elements in the form of sum of powers-of-two; thus making the filter architecture hardware friendly. Finally, the DE-optimized 2-D filter has been used to reduce the effect of Gaussian noise of different intensities from three test images and the its performance has been compared with other approaches in terms of various parameters like peak signal-to-noise ratio (PSNR), structural similarity index measure (SSIM), image enhancement factor (IEF) and image quality index (IQI).

2 Notion about two-dimensional FIR filter

Two-dimensional FIR filter, used for processing images of various kinds, is always characterized by its mask coefficients $h(m,n)$ defined for $-M \le m \le M$ and $-N \le n \le N$. Frequency response of this $(2M+1)\ X\ (2N+1)$ image filter is therefore given by [7, 12]:

$$H(\omega_u,\ \omega_v) = \sum_{m=-M}^{M} \sum_{n=-N}^{N} h(m,n) e^{-j(m\omega_u + n\omega_v)}\ where\ \omega_u = \frac{2\pi u}{M} and\, \omega_v = \frac{2\pi v}{N} \tag{1}$$

As can be implicitly seen from (1), image filter of given size requires $\mathcal{M}_1 = (2M+1).(2N+1)$ number of mask coefficients to synthesize. With the addition of some constraints imposed as the horizontal and vertical equivalence of the mask coefficients, it will show symmetry about the diagonals. This may be mathematically outlined as follows:

$$h(m,n) = h(n,m)\ and\ M = N \tag{2}$$

With the constraints in (2), there has been a significant reduction in the total number of unique coefficients needed to identify the mask set. More specifically, the condition in (2) requires that the coefficient values therefore need to be specified only for $0 \le m \le M$ and $0 \le n \le m$. As a matter of fact, this formulation is in need of at most $\mathcal{M}_2 = \frac{(M+1)(M+2)}{2}$ number of distinct coefficients to be synthesized. Compared to the traditional approach, this encoding technique will lead to a reduction in mask coefficients by a factor of $\mathcal{M} = \frac{2(2M+1)^2}{(M+1)(M+2)}$. For very large value of M, value of $\mathfrak{W}$ approaches to 8. Construction of an arbitrary filter mask of size 5×5 may look like as follows:

$$\mathbb{H}_{5X5} = \begin{bmatrix} \phi & \theta & \gamma & \theta & \phi \\ \theta & \delta & \beta & \delta & \theta \\ \gamma & \beta & \alpha & \beta & \gamma \\ \theta & \delta & \beta & \delta & \theta \\ \phi & \theta & \gamma & \theta & \phi \end{bmatrix} = \Theta_5(\alpha,\beta,\gamma,\delta,\theta,\phi), \tag{3}$$

where $\Theta_{(2M+1)}$ is considered as a function to map $\mathcal{M}_2$ coefficients into a $(2M+1)\,X\,(2M+1)$ matrix.

It can be clearly seen from (3) that 25 positions in the filter mask have been completely occupied by 6 coefficients only leading to $\mathfrak{W} = 4.167$. Hardware efficiency of the image filter may further be enhanced by encoding the mask coefficients as sum of powers-of-two so that multiplication with the image pixels may simply be carried out by means of shifted additions only. Mask coefficient may therefore mathematically be represented by:

$$h(m,n) = \sum_{i=0}^{\Delta-1} c_i(m,n)2^{-i} \quad \forall -M \le m, n \le M, \tag{4}$$

where $c_i(m,n) \in \mathbb{B} = \{0,\ 1\}$ and the term Δ is known as the word-length of the coefficient. Selection of these binary coefficients from the set $\mathbb{B}$ is a problem of optimization and has been dealt in this paper with the aid of a one of the most powerful evolutionary computational techniques.

3 Differential evolution algorithm

The theory of optimization technique has proved its supremacy in a wide variety of science and engineering research problems over a number of years. Inability of derivative based linear optimization techniques in locating the global minima through a non-linear rough surface has been overcome in the later part of the last century through the invention of a number of intelligent optimization methods guided by genetic and social behavior of animals [3], [4].

Differential Evolution (DE) is a multi-objective, population-based search algorithm employed for finding out the optimal D-dimensional solution from a search space consisting of P number of potential solutions which is related to D as $5D \le P \le 10D$. The set of vectors at any iteration 'G' can be represented as $\mathbb{S}_G = \left\{x_{i,j}^G\right\}$; $\forall\ i \in \rho = \{1,2,3,\ldots..,P\}$ *and* $j = \{1,2,3,\ldots..,D\}$ where $x_{i,j}^G$ identifies the j^{th} element (gene) of i^{th} member (chromosome) at iteration G.

In order to generate new parameter vector for the next generation, DE uses a special type of differential operator where the weighted difference between two parameter vector of current generation is added to a third vector, yielding the mutant vector for the next iteration as [4]:

$$v_{i,j}^{G+1} = x_{r_1,j}^G + F.\left(x_{r_2,j}^G - x_{r_3,j}^G\right) \qquad \forall i, r_1, r_2, r_3 \in \rho \textit{ and } i \ne r_1 \ne r_2 \ne r_3 \textit{ with} \tag{5}$$
$$j = \{1,2,3,\ldots..,D\}$$

Since the above process perturbs the current parameter vector by using three other distinct parameter vectors, it is quite similar to the genetic mutation process where the genomes of chromosomes undergo changes and accordingly the process is called as 'mutation' mechanism. The parameter 'F', which acts as amplification factor in (5), has proved to play a significant role in convergence behavior of DE and rightly termed as 'weighting factor'. It is a real and constant value that can assume values from the range [0, 2]. However, its value is chosen as 0.5 in most of the applications.

Table 1 Analysis of computational complexity of the proposed algorithm

Size of population	Number of iterations					
	10	20	30	40	50	100
20	28 s	46 s	1 min 10 s	1 min 39 s	1 min 46 s	3 min 43 s
30	34 s	1 min 7 s	2 min 2 s	2 min 36 s	2 min 45 s	5 min 33 s
40	46 s	1 min 29 s	2 min 25 s	3 min 22 s	3 min 34 s	7 min 33 s
50	58 s	1 min 52 s	3 min 20 s	4 min 6 s	4 min 38 s	9 min 15 s

Diversity of the perturbed vector is enhanced in the next step of DE where, depending upon some random parameters, one or more genomes of the mutant vector of the present generation enter the target vector $U_i^{G+1}=\{u_{i,j}^{G+1}\}\ \forall\ j=\{1,2,3,\ldots.., D\}$ for the next generation [3, 17, 18]:

$$u_{i,j}^{G+1} = \begin{cases} v_{i,j}^{G+1} & if \quad rand_{i,j} \leq \quad CR \quad or \quad j = randn_i \\ x_{i,j}^{G} & if \quad rand_{i,j} > CR \quad or \quad j = randn_i \end{cases} \quad \forall i \in \rho \, and \, j = \{1,2,3\ldots,D\} \tag{6}$$

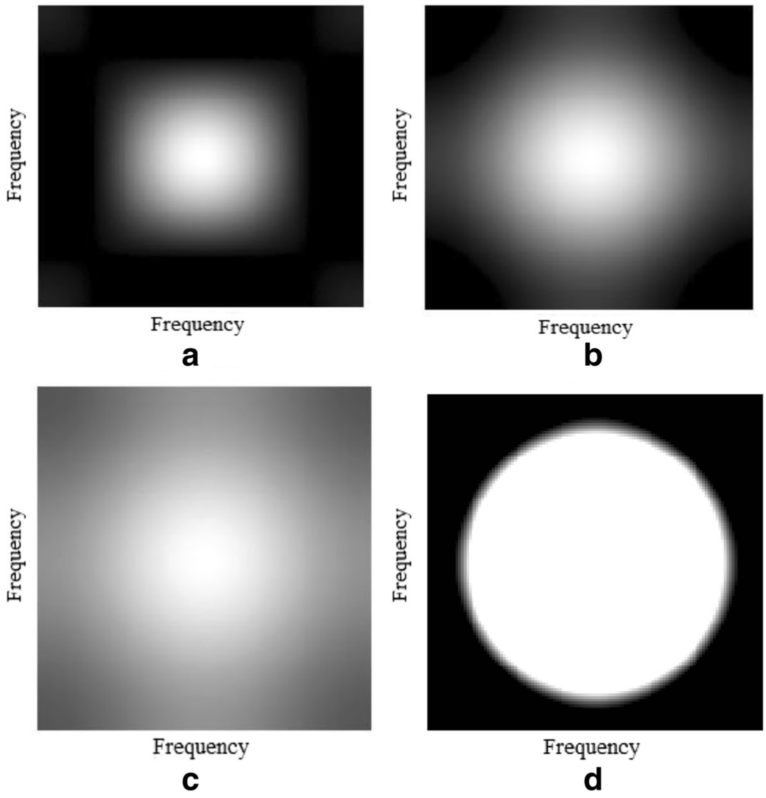

Fig. 1 Frequency response of **a** mean **b** circular averaging **c** Gaussian **d** proposed filter

Table 2 Comparison in terms of PSNR (dB) resulting from various filters at different noise intensities for Lena image

Filter type	Standard deviation of Gaussian noise								
	0.1	0.15	0.2	0.25	0.3	0.35	0.4	0.45	0.5
Mean	19.42	16.28	13.93	12.09	10.62	9.4	8.39	7.53	6.83
Disk	19.24	16.17	13.87	12.06	10.59	9.38	8.36	7.52	6.82
Gaussian	18.53	15.81	13.65	11.92	10.49	9.3	8.31	7.48	6.79
Median	19.22	16.13	13.79	11.96	10.48	9.25	8.22	7.35	6.63
Proposed	23.84	24.45	22.32	19.64	17.34	15.49	13.99	12.76	11.76

Equation (6) involves a control parameter CR, called 'crossover probability' which actually takes care of the number of genomes from the mutant vector that may be allowed to enter as element in the target vector. Proper care has to be taken during the selection of this parameter which is normally chosen from the set [0, 1].

Process of selection is carried out in the final step of DE where it is decided whether or not the target vector of the current generation may get entered as a parameter vector for the next generation $X_i^{G+1}=\{x_{i,j}^{G+1}\}\ \forall\ j=\{1,2,3,\ldots., D\}$. It involves a comparison between the target vector and the present parameter vector using one greedy criterion. The comparison is based on proper formulation of an objective or cost function $\varphi(.)$ as outlined in the following equation [4]:

$$X_i^{G+1} = \begin{cases} U_i^{G+1} & iff\ \ \phi\left(X_i^G\right) \geq \phi\left(U_i^{G+1}\right) \\ X_i^G & iff\ \ \phi\left(X_i^G\right) < \phi\left(U_i^{G+1}\right) \end{cases} \tag{7}$$

The process of mutation, cross-over or recombination and selection continues in an iterative way until the maximum number of iteration is exhausted or the optimum solution has been achieved.

4 Design formulation

This section briefly describes our novel algorithm for the design of two-dimensional multiplier-less low-pass FIR filter using Differential Evolution algorithm. Our design objective has

Table 3 Comparison in terms of SSIM resulting from various filters at different noise intensities for Lena image

Filter type	Standard deviation of Gaussian noise								
	0.1	0.15	0.2	0.25	0.3	0.35	0.4	0.45	0.5
Mean	0.9284	0.9061	0.8799	0.8515	0.8208	0.7875	0.7503	0.7075	0.6575
Disk	0.9148	0.8927	0.8668	0.8385	0.808	0.7752	0.7385	0.6966	0.6473
Gaussian	0.8842	0.8628	0.8377	0.8105	0.7814	0.7498	0.715	0.675	0.6283
Median	0.949	0.9269	0.9012	0.8736	0.8441	0.8117	0.7746	0.7321	0.6816
Proposed	0.9331	0.9082	0.9	0.884	0.8605	0.8291	0.789	0.7393	0.679

Table 4 Comparison in terms of IEF resulting from various filters at different noise intensities for Lena image

Filter type	Standard deviation of Gaussian noise								
	0.1	0.15	0.2	0.25	0.3	0.35	0.4	0.45	0.5
Mean	1.016	1.013	1.012	1.011	1.01	1.009	1.009	1.008	1.008
Disk	1.664	1.328	1.191	1.123	1.085	1.061	1.045	1.034	1.026
Gaussian	1.413	1.221	1.133	1.087	1.06	1.043	1.032	1.024	1.018
Median	1.006	0.9979	0.9895	0.9828	0.9789	0.975	0.9698	0.9649	0.9633
Proposed	4.781	8.915	8.335	6.43	5.134	4.33	3.809	3.455	3.205

been regarded as the minimization of error between the frequency response of 2-D ideal low-pass filter and that of the proposed one through evolutionary optimization technique. This has been mathematically formulated as outlined below:

$$\mathfrak{C}_i = \sum_{u=1}^{\aleph} \sum_{v=1}^{\aleph} \left| W(\omega_u, \omega_v) - H_i(\omega_u, \omega_v) \right|^2, \tag{8(a)}$$

where $\aleph$ is the number of frequency samples in vertical and horizontal direction, $H_i(\omega_u,\omega_v)$ is the normalized frequency response of the i^{th} mask coefficient $h_i(m,n)$, related as in (1) and $W(\omega_u,\omega_v)$ is the frequency response of ideal 2-D low-pass filter, defined as:

$$W(\omega_u, \omega_v) = \begin{cases} 1 \ for \ \sqrt{\left(u - \frac{\aleph}{2}\right)^2 + \left(v - \frac{\aleph}{2}\right)^2} \leq z \\ 0 \ for \ \sqrt{\left(u - \frac{\aleph}{2}\right)^2 + \left(v - \frac{\aleph}{2}\right)^2} > z \end{cases} \tag{8(b)}$$

Since, evolutionary computation technique has been judiciously used in this paper for the design of multiplier-less 2-D low-pass filter, mask coefficients have been encoded as chromosome which are allowed to take part in subsequent genetic operations like mutation, cross-over and selection. It has been already established that an $M\ X\ M$ filter mask is in need of at most $\mathcal{M}_2$ number of distinct coefficients each of which are encoded by at most Δ bits. As a matter of fact, the entire set of potential solution is populated by $\mathcal{P} = P.\mathcal{M}_2$ number of chromosomes, each of length Δ and stored in the set $\mathbb{I} = \{\mathcal{C}_i\},\ i \in \mathbb{P} = \{1, 2, 3, \ldots.., \mathcal{P}\}$, where the arbitrary chromosome $\mathcal{C}_i$ may be represented as:

Table 5 Comparison in terms of IQI resulting from various filters at different noise intensities for Lena image

Filter type	Standard deviation of Gaussian noise								
	0.1	0.15	0.2	0.25	0.3	0.35	0.4	0.45	0.5
Mean	0.9539	0.9314	0.9051	0.8763	0.8455	0.812	0.7746	0.7314	0.6803
Disk	0.9487	0.9268	0.9012	0.8731	0.8433	0.8108	0.7747	0.7329	0.6835
Gaussian	0.9225	0.9015	0.877	0.8504	0.8222	0.7915	0.7575	0.7184	0.6714
Median	0.9486	0.9266	0.9008	0.8732	0.8438	0.8111	0.7739	0.731	0.68
Proposed	0.9362	0.9367	0.9285	0.9127	0.8892	0.8572	0.8162	0.7647	0.7019

Table 6 Comparison in terms of PSNR (dB) resulting from various filters at different noise intensities for Moon image

Filter type	Standard deviation of Gaussian noise								
	0.1	0.15	0.2	0.25	0.3	0.35	0.4	0.45	0.5
Mean	19.05	16.11	13.8	11.97	10.44	9.14	8.03	7.07	6.24
Disk	18.96	16.04	13.77	11.92	10.41	9.11	8	7.05	6.21
Gaussian	18.39	15.72	13.56	11.78	10.3	9.03	7.95	6.99	6.17
Median	19.12	16.07	13.78	11.91	10.37	9.07	7.95	6.96	6.11
Proposed	23.07	20.96	18.56	16.43	14.65	13.14	11.83	10.74	9.77

$$\mathcal{C}_i = \left[c_{i,0}\ \ c_{i,1}\ \ c_{i,2}\ \ldots..c_{i,\Delta-1}\right]\ \forall\ i\in\mathbb{P} \tag{9}$$

In connection to the execution of conventional DE algorithm, members from the set $\mathbb{I}$ have been allowed to take part in subsequent genetic operations as in (5), (6) and (7) and new sets of vectors, namely $\mathbb{D} = \{\mathcal{D}_i\}$, $\mathbb{T} = \{\mathcal{T}_i\}$, $\mathbb{S} = \{\mathcal{S}_i\}$, $i\in\mathbb{P}$, are formulated accordingly; where $\mathcal{D}_i,\ \mathcal{T}_i$ *and* $\mathcal{S}_i$ are known as donor, target and selected vectors respectively. These vectors are related to each other as:

$$\mathcal{D}_i = \mathfrak{W}\left\{\mathcal{C}_j,\ \mathcal{C}_k, \mathcal{C}_l\right\},\ with\ i\neq j\neq k\neq l\ and\ i,j,k,l\in\mathbb{P} \tag{10}$$

$$\mathcal{T}_i = \mathfrak{R}\{\mathcal{D}_i, \mathcal{C}_i\}\ \forall\ i\in\mathbb{P} \tag{11}$$

$$\mathcal{S}_i = \mathfrak{S}\left\{\mathcal{C}_i^{'},\ \mathcal{T}_i^{'}\right\}\ \forall\ i\in\rho \tag{12}$$

$\mathfrak{W}$, $\mathfrak{R}$ *and* $\mathfrak{S}$ symbolically identify the mutation, recombination (cross-over) and selection operations respectively. It is to be noticed that the parameters undergone through the process of selection are symbolized as $\mathcal{C}_i^{'}$ *and* $\mathcal{T}_i^{'}$ which can be obtained from $\mathcal{C}_i$ *and* $\mathcal{T}_i$ respectively as:

$$\mathrm{c}_i = \sum_{j=0}^{\Delta-1} \mathcal{C}_{i,j} 2^{-j}\ \forall\ i\in\mathbb{P} \tag{13(a)}$$

Table 7 Comparison in terms of SSIM resulting from various filters at different noise intensities for Moon image

Filter type	Standard deviation of Gaussian noise								
	0.1	0.15	0.2	0.25	0.3	0.35	0.4	0.45	0.5
Mean	0.8968	0.8439	0.788	0.7345	0.6845	0.6394	0.5982	0.5608	0.5264
Disk	0.8867	0.8338	0.7784	0.7253	0.6755	0.6308	0.5903	0.5539	0.5196
Gaussian	0.8623	0.8103	0.756	0.7044	0.6565	0.6129	0.5738	0.5382	0.5049
Median	0.9033	0.847	0.7898	0.7355	0.6855	0.6404	0.5995	0.563	0.5301
Proposed	0.9146	0.8952	0.8628	0.8232	0.7816	0.7397	0.6993	0.6581	0.6181

Table 8 Comparison in terms of IEF resulting from various filters at different noise intensities for Moon image

Filter type	Standard deviation of Gaussian noise								
	0.1	0.15	0.2	0.25	0.3	0.35	0.4	0.45	0.5
Mean	1.581	1.319	1.197	1.134	1.096	1.073	1.058	1.046	1.039
Disk	1.547	1..302	1.187	1.125	1.089	1.066	1.051	1.041	1.034
Gaussian	1.359	1.207	1.131	1.089	1.064	1.048	1.037	1.029	1.023
Median	1.604	1.316	1.314	1.188	1.122	1.084	1.055	1.021	1.009
Proposed	3.976	4.052	3.583	3.175	2.893	2.688	2.542	2.43	2.342

$$\mathcal{C}_i^{'} = \Theta_{(2M+1)}\left\{\mathrm{c}_{\mathcal{M}_2(i-1)+1},\ \mathrm{c}_{\mathcal{M}_2(i-1)+2},\ \mathrm{c}_{\mathcal{M}_2(i-1)+3},\ \ldots..,\ \mathrm{c}_{\mathcal{M}_2 i}\right\}\ \forall\ i\in\rho \tag{13(b)}$$

$$\tau_i = \sum_{j=0}^{\Delta-1} \mathcal{T}_{i,j} 2^{-j}\ \forall\ i\in\mathbb{P} \tag{14(a)}$$

$$\mathcal{T}_i^{'} = \Theta_{(2M+1)}\left\{\tau_{\mathcal{M}_2(i-1)+1},\ \tau_{\mathcal{M}_2(i-1)+2},\ \tau_{\mathcal{M}_2(i-1)+3},\ \ldots..,\tau_{\mathcal{M}_2 i}\right\}\ \forall\ i\in\rho \tag{14(b)}$$

Since DE is a population-based algorithm, it yields a number of solutions at the end of every iteration with different cost functional value. Optimum mask coefficient $\mathbb{H}^{opt}_{(2M+1)X(2M+1)}$ is eventually constructed from the best alternative $\mathcal{S}_{opt}$ which is extracted from the set $\mathbb{S}$ and for which $\mathfrak{C}_{opt}<\mathfrak{C}_i\ \ \forall\ i\in\rho$. This may have its mathematical illustration as:

$$\mathbb{H}^{opt}_{(2M+1)X(2M+1)} = \Theta_{(2M+1)}\left\{\mathcal{S}_{\mathcal{M}_2(opt-1)+1}, \mathcal{S}_{\mathcal{M}_2(opt-1)+1}, \mathcal{S}_{\mathcal{M}_2(opt-1)+1}, \ldots.., \mathcal{S}_{\mathcal{M}_2(opt-1)+1}\right\} \tag{15}$$

5 Results

Application of evolutionary computation techniques towards the optimization of real variables like filter (mask) coefficient has been seriously challenged by its computational complexity. As a matter of fact, analysis of computation time is given the highest priority before incorporating those optimization techniques in practice. In connection to this, computational complexity of the proposed algorithm in synthesizing 3×3 filter mask has

Table 9 Comparison in terms of IQI resulting from various filters at different noise intensities for Moon image

Filter type	Standard deviation of Gaussian noise								
	0.1	0.15	0.2	0.25	0.3	0.35	0.4	0.45	0.5
Mean	0.9048	0.8499	0.7933	0.7392	0.7392	0.644	0.6031	0.5663	0.5322
Disk	0.9024	0.8475	0.7912	0.7912	0.7367	0.6424	0.6019	0.5654	0.5316
Gaussian	0.8844	0.8294	0.7735	0.7735	0.7205	0.6287	0.5895	0.5538	0.5212
Median	0.9032	0.8465	0.7893	0.7893	0.7352	0.6398	0.5992	0.563	0.5297
Proposed	0.9293	0.9074	0.8728	0.8728	0.8323	0.7476	0.7057	0.665	0.624

Table 10 Comparison in terms of PSNR (dB) resulting from various filters at different noise intensities for MRI image

Filter type	Standard deviation of Gaussian noise								
	0.1	0.15	0.2	0.25	0.3	0.35	0.4	0.45	0.5
Mean	18.43	15.89	13.8	12.1	10.69	9.52	8.52	7.68	6.94
Disk	18.76	16.04	13.89	12.14	10.72	9.52	8.53	7.67	6.94
Gaussian	18.46	15.85	13.76	12.06	10.66	9.48	8.49	7.64	6.91
Median	18.52	15.83	13.68	11.93	10.5	9.3	8.29	7.45	6.74
Proposed	19.92	19.35	18.01	16.44	14.94	13.61	12.45	11.45	10.58

been studied thoroughly in this section for four different sizes of population. Entire simulation has been carried out by means of MATLAB 7.10 software in an Intel Pentium 4 CPU with 1 GB of RAM. Complete set of computation time has been summarized in Table 1 below.

From Table 1, it can be explicitly observed that the computation time increases linearly with the total number of iterations. Moreover, dependence of simulation time on the size of population is also found to maintain linear relationship. Optimum design of such 3×3 mask with coefficients encoded in the form of powers-of-two has been accomplished using a population size of 40 at a total number of iterations of 50.

Performance of the DE-optimized multiplier-less 2-D (DEML2D) filter has been analyzed from various perspectives in this article. To start with, frequency response of such a 3×3 filter has been depicted in Fig. 1 below along with that of other low-pass two-dimensional filter of similar order.

Figure 1 unambiguously suggests the effectiveness of the proposed multiplier-less DE-optimized filter in allowing the low frequency components of an image while eliminating its high frequency substituent like noise to a significant extent. This has been readily identified from Fig. 1(d) that the frequency response of the proposed filter is distinctively divided into two regions, namely white and black. In connection to this, white area corresponds to the frequency components which are essentially passed by the filter and black area corresponds to those frequency components completely blocked by it. On the other hand, it merely contains any grey variation and thus significantly enhanced the sharpness of the filter. However, the frequency response of mean, circular and Gaussian filter in particular consists of grey levels which results in considerable blurring of the processed image.

Table 11 Comparison in terms of SSIM resulting from various filters at different noise intensities for MRI image

Filter type	Standard deviation of Gaussian noise								
	0.1	0.15	0.2	0.25	0.3	0.35	0.4	0.45	0.5
Mean	0.9076	0.8775	0.843	0.8064	0.7697	0.7331	0.6973	0.6608	0.6238
Disk	0.8986	0.8696	0.8355	0.7995	0.7634	0.728	0.6924	0.657	0.6201
Gaussian	0.8837	0.8545	0.8215	0.7865	0.7512	0.7169	0.6827	0.6484	0.6124
Median	0.9405	0.9066	0.8688	0.8292	0.7898	0.7514	0.7129	0.6754	0.6363
Proposed	0.8879	0.8833	0.868	0.8444	0.8155	0.782	0.7456	0.7053	0.6613

Table 12 Comparison in terms of IEF resulting from various filters at different noise intensities for MRI image

Filter type	Standard deviation of Gaussian noise								
	0.1	0.15	0.2	0.25	0.3	0.35	0.4	0.45	0.5
Mean	1.319	1.194	1.126	1.086	1.062	1.047	1.037	1.032	1.028
Disk	1.422	1.241	1.149	1.099	1.069	1.051	1.039	1.032	1.027
Gaussian	1.323	1.185	1.117	1.078	1.054	1.04	1.03	1.024	1.02
Median	1.348	1.178	1.095	1.046	1.016	0.9967	0.9849	0.9798	0.9796
Proposed	1.856	2.655	2.965	2.946	2.825	2.688	2.564	2.459	2.371

While the frequency characteristics of different 2-D low-pass filters can provide qualitative information regarding the efficiency of filtering process, a more realistic analysis may be carried out in terms of various performance parameters which are directly related to the quality of the filtered image. Denoising performance of the filter is generally evaluated in terms of peak signal-to-noise ratio (PSNR), structural similarity index measure (SSIM) [24], image enhancement factor (IEF) [5, 15] and image quality index (IQI) [23] which are defined as follows:

$$PSNR = 20log_{10}\left(\frac{\max_{i,j}\{I(i,j)\}}{\sqrt{\frac{1}{RC}\sum_{i=1}^{R}\sum_{j=1}^{C}\{I(i,j)-F(i,j)\}^2}}\right) \tag{16}$$

$$SSIM(I,F) = \frac{(2\mu_I\mu_F + K_1)(2\sigma_{IF} + K_2)}{(\mu_I^2 + \mu_F^2 + K_1)(\sigma_I^2 + \sigma_F^2 + K_2)} \tag{17}$$

$$IEF = \frac{\sum_{i=1}^{R}\sum_{j=1}^{C}\{N(i,j)-I(i,j)\}^2}{\sum_{i=1}^{R}\sum_{j=1}^{C}\{F(i,j)-I(i,j)\}^2} \tag{18}$$

$$\begin{aligned} IQI &= corr(I,F).lum(I,F).cont(I,F) \\ where\ ,\ corr\ (I,F) &= \frac{\sigma_{IF}}{\sigma_I\sigma_F} \\ lum\ (I,F) &= \frac{2\mu_I\mu_F}{(\mu_I^2+\mu_F^2)} \\ and\ cont\ (I,F) &= \frac{2\sigma_I\sigma_F}{(\sigma_I^2+\sigma_F^2)} \end{aligned} \tag{19}$$

Table 13 Comparison in terms of IQI resulting from various filters at different noise intensities for MRI image

Filter type	Standard deviation of Gaussian noise								
	0.1	0.15	0.2	0.25	0.3	0.35	0.4	0.45	0.5
Mean	0.9386	0.9061	0.8696	0.8306	0.7919	0.7538	0.7159	0.678	0.6386
Disk	0.9449	0.9119	0.8746	0.8358	0.7969	0.7583	0.7206	0.682	0.6429
Gaussian	0.9397	0.9068	0.8696	0.8311	0.7928	0.7546	0.7171	0.6791	0.64
Median	0.9403	0.9065	0.8687	0.8292	0.7898	0.751	0.7129	0.6748	0.6357
Proposed	0.9279	0.921	0.9028	0.8766	0.8449	0.8086	0.7691	0.7251	0.6786

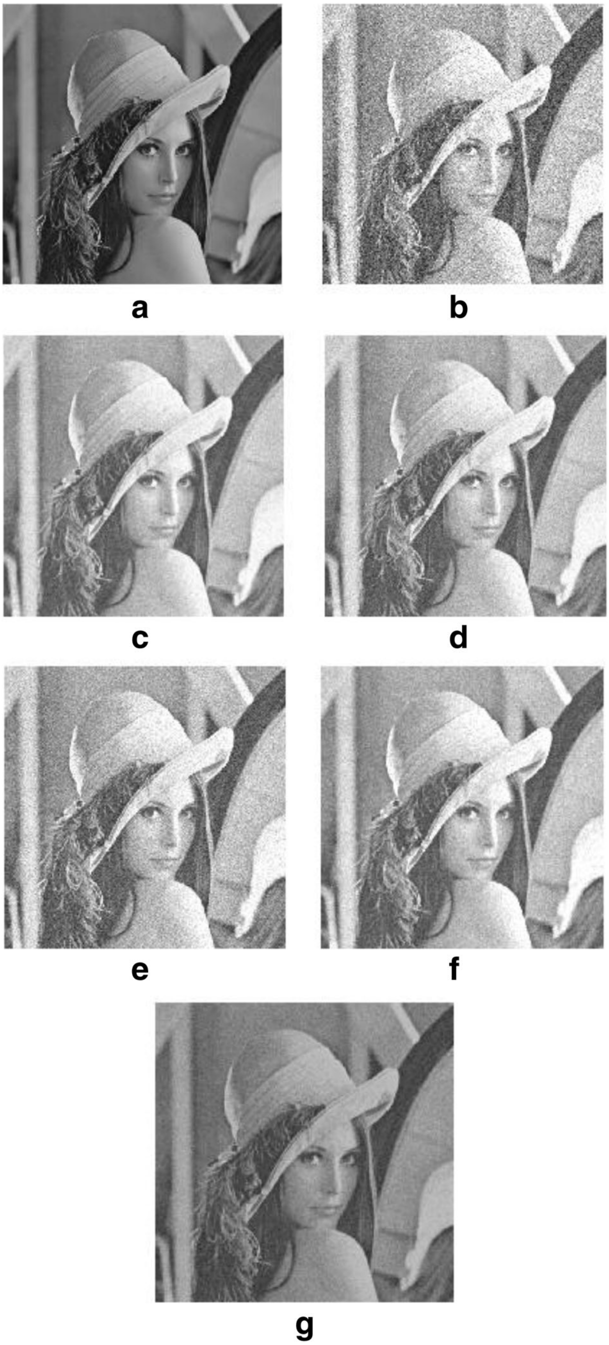

Fig. 2 **a** Original **b** Noisy (Gaussian noise with σ=0.25) **c** Mean-filtered **d** Circular-filtered **e** Gaussian-filtered **f** Median-filtered **g** Proposed DEML2D FIR-filtered Lena image

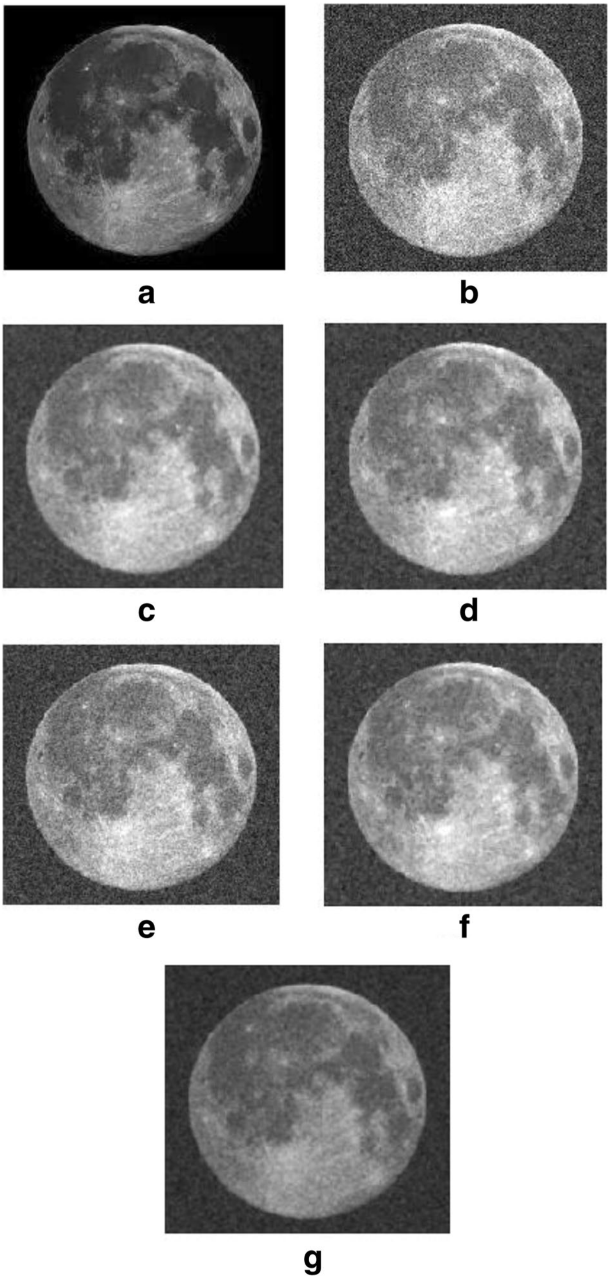

Fig. 3 **a** Original **b** Noisy (Gaussian noise with σ=0.25) **c** Mean-filtered **d** Circular-filtered **e** Gaussian-filtered **f** Median-filtered **g** Proposed DEML2D FIR-filtered Moon image

Where, $I(i,j)$, $N(i,j)$ *and* $F(i,j)$ represent the input image, noisy image and filtered image of dimension $R\ X\ C$ respectively. Parameters μ *and* σ indicate the mean intensity and standard deviation from the mean intensity respectively and defined as:

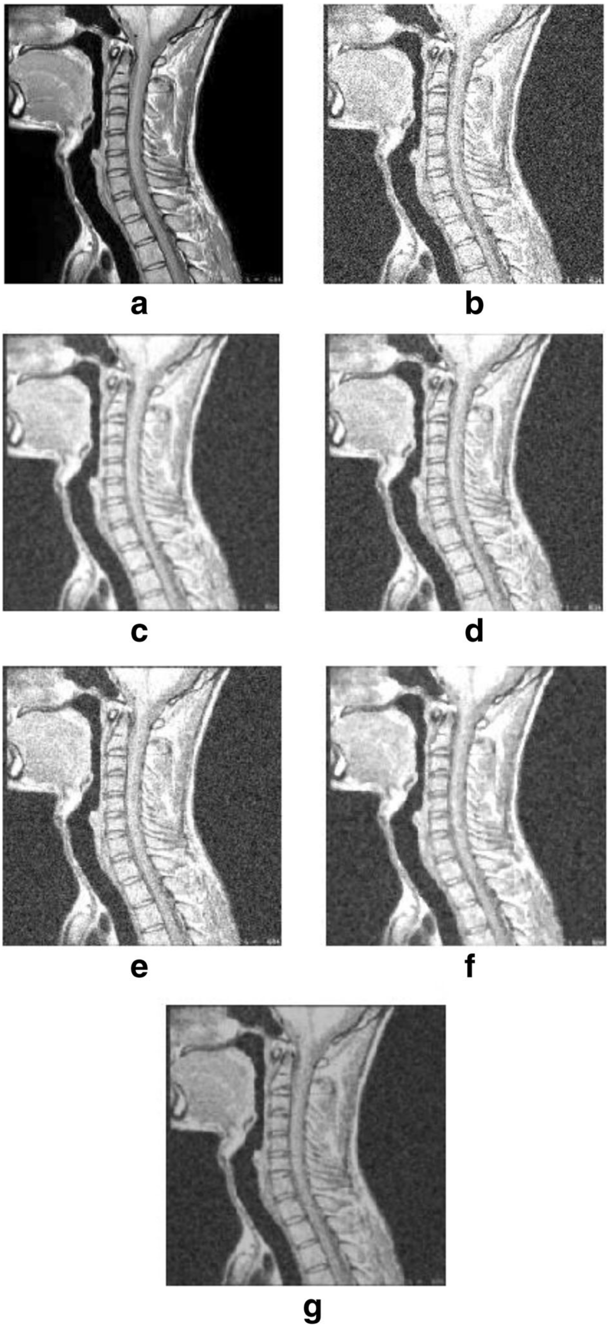

Fig. 4 **a** Original **b** Noisy (Gaussian noise with σ=0.25) **c** Mean-filtered **d** Circular-filtered **e** Gaussian-filtered **f** Median-filtered **g** Proposed DEML2D FIR-filtered MRI image

$$\mu_X = \frac{1}{RC}\sum_{i=1}^{R}\sum_{j=1}^{C} X(i,j)\ where X = I\ or\ F \tag{20}$$

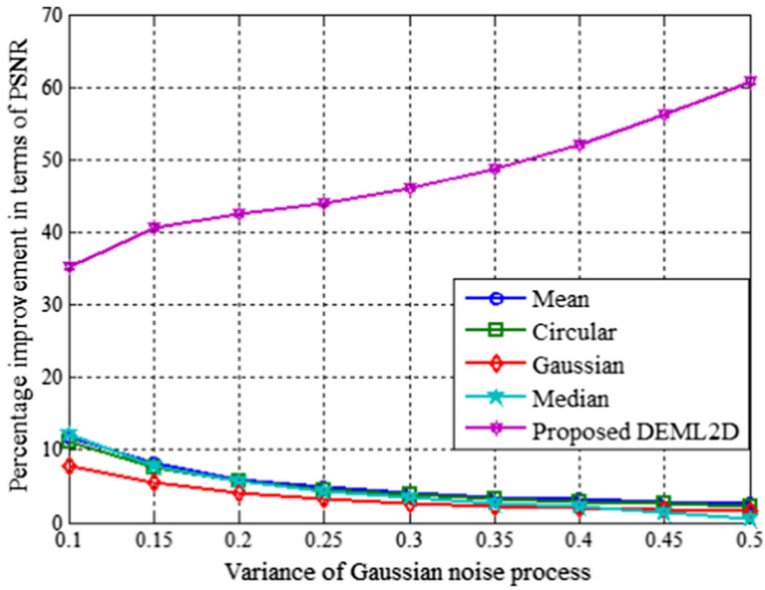

Fig. 5 Percentage improvement of filtered Moon image in terms of PSNR

$$\sigma_X = \sqrt{\frac{1}{RC}\sum_{i=1}^{R}\sum_{j=1}^{C}\{X(i,j)-\mu_X\}^2} \text{ where } X = I \text{ or } F \tag{21}$$

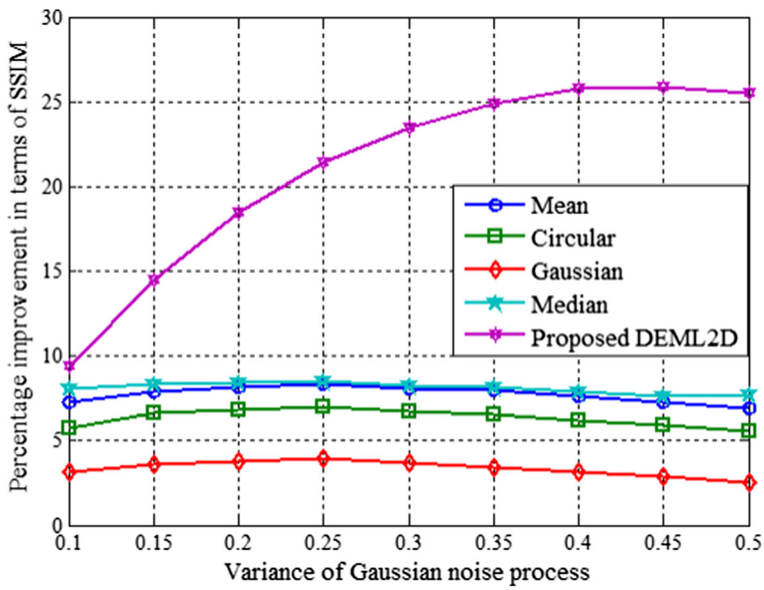

Fig. 6 Percentage improvement of filtered Moon image in terms of SSIM

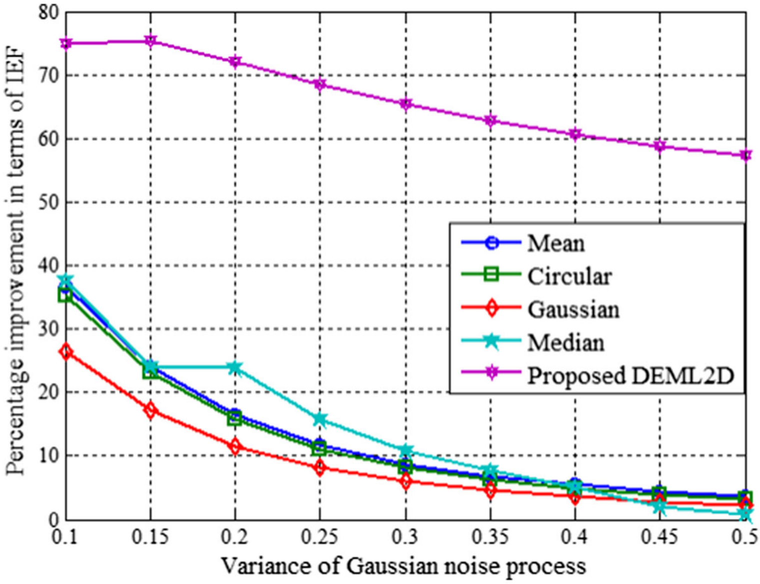

Fig. 7 Percentage improvement of filtered Moon image in terms of IEF

$$\sigma_{IF} = \sqrt{\frac{1}{RC}\sum_{i=1}^{R}\sum_{j=1}^{C} \left|I(i,j)-\mu_I\right| \left|F(i,j)-\mu_F\right|} \tag{22}$$

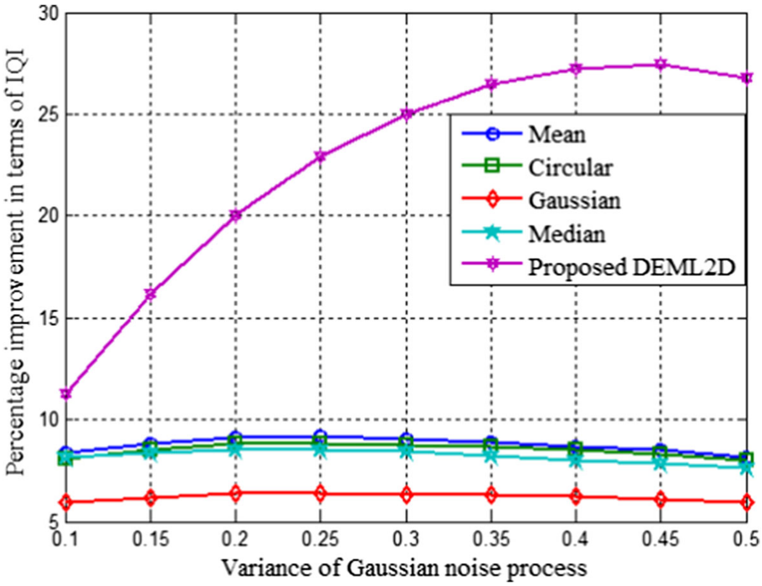

Fig. 8 Percentage improvement of filtered Moon image in terms of IQI

Based on the above parameters, performance of the low-pass filter in eliminating Gaussian noise from three different test images, namely Lena, Moon and MRI, have been measured and accordingly the numerical values have been listed in Tables 2, 3, 4, 5, 6, 7, 8, 9, 10, 11, 12 and 13 below. Original, noisy and filtered images have also been included in Figs. 2, 3 and 4 for the purpose of visual comparison.

Looking at the entries in Tables 2, 3, 4, 5, 6, 7, 8, 9, 10, 11, 12 and 13, it can be clearly inferred that irrespective of the intensity of Gaussian noise, the performance of the proposed DEML2D FIR filter in eliminating the noise component and thereby restoring the image characteristics is comparatively better than other approaches as mentioned in the article. This has been substantiated by means of a number of performance parameters like PSNR, SSIM, IEF and IQI. However for space constraint, the percentage improvement in terms of those parameters, as achieved with different filtering algorithms, with respect to noisy Moon image only had been depicted in Figs. 5, 6, 7 and 8 below.

Figure 5, 6, 7 and 8 explicitly demonstrates the usefulness of the proposed DEML2D filter over other approaches in eliminating the effect of Gaussian noise from the Moon image. Irrespective of the performance parameters considered and the variances of the Gaussian noise process, the percentage improvement achieved with the proposed DEML2D filter is always higher than the other denoising algorithms. It can also be inspected that except the parameter IEF, percentage improvement achieved with our proposed filter in terms of other parameters like PSNR, SSIM and IQI monotonically increases with the variance of the noise process unlike the other filtering mechanisms for which the improvement remains either insensitive (in terms of SSIM and IQI) to the value of the variance or reduces (in terms of PSNR and IEF) with the increase of variance. Moreover, in terms of PSNR, SSIM and IQI, the maximum improvement achieved with the other four approaches is limited to 10 % only while the proposed approach yields at most 60 %, 26 % and 28 % improvement respectively. However, with respect to IEF, DEML2D results in approximately 75 % improvement for a noise variance of 0.1 while the same achieved with other approaches is strictly less than 40 %.

Performance of the proposed filter has also been compared with respect to some recent developments in image filter design. In this regard, comparative analysis has been carried out on three test images, namely Lena, Moon & Peppers and the values for SSIM at three distinct noise intensities have been measured and subsequently listed in Table 14, 15 and 16 below respectively.

Looking at the entries in Tables 14, 15 and 16, supremacy of the proposed DE-based 2-D filter design can be well established as it always yields higher SSIM value compared to the other state-of-the-art filter design strategies. Amongst the rest, image filter designed with the aid of DEPSO-based approach produces the best result. It has also been observed that the

Table 14 Comparison in terms of SSIM at different noise intensities for Lena image

Type of filter	Standard deviation of Gaussian noise		
	0.1	0.2	0.3
Bilateral filtering (BF) [21]	0.798	0.7552	0.5877
Stochastic denoising (SD) [6]	0.852	0.534	0.3532
DEPSO-based design [8]	0.8692	0.7702	0.7004
Proposed DEML2D	0.9331	0.9	0.8605

Table 15 Comparison in terms of SSIM at different noise intensities for Moon image

Type of filter	Standard deviation of Gaussian noise		
	0.1	0.2	0.3
Bilateral filtering (BF) [21]	0.6306	0.6453	0.5594
Stochastic denoising (SD) [6]	0.8567	0.5873	0.3843
DEPSO-based design [8]	0.8545	0.7435	0.6654
Proposed DEML2D	0.9146	0.8628	0.7816

performance of our proposed design improves with an increase in the intensity of Gaussian noise i.e. with its standard deviation. As for example, SSIM improvements of the proposed design with respect to [8] in Lena image turn out to be 7.35, 16.85 and 22.86 % at noise standard deviation of 0.1, 0.2 and 0.3 respectively. Similar improvements in Moon and Peppers image have been calculated as 7.03, 16.05 & 17.46 and 5.59, 11.6 & 14.24 % respectively.

6 Conclusions

In this communication, we have proposed a novel design strategy of multiplier-less two-dimensional low-pass denoising filter with the aid of Differential Evolution algorithm. Mask coefficients of the filter have been encoded in the form of sum of powers-of-two. Proposed filter has been used to reduce the effect of Gaussian noise of different intensities from digital images. Performance of the proposed DEML2D filter in denoising application has been studied on few test images with respect to some relevant parameters like PSNR, SSIM, IEF and IQI. In connection to this, superiority of our design has been established over some conventional image filter and few state-of-the-arts image denoising algorithms. Proposed algorithm has been formulated for a fixed setting of the control parameters of DE like weighting factor, cross-over probability. Since the performance of DE is influenced by the choice of its control parameters; future research may be carried out by properly selecting the optimum values for these parameters. Moreover, the existing algorithm may be modified by choosing the control parameters in an adaptive way.

Table 16 Comparison in terms of SSIM at different noise intensities for Peppers image

Type of filter	Standard deviation of Gaussian noise		
	0.1	0.2	0.3
Bilateral filtering (BF) [21]	0.8429	0.7851	0.5948
Stochastic denoising (SD) [6]	0.8562	0.5196	0.3372
DEPSO-based design [8]	0.8913	0.8087	0.7422
Proposed DEML2D	0.9411	0.9025	0.8479

References

1. Bhadouria VS, Ghoshal D, Siddiqi AH (2013) A new approach for high density saturated impulse noise removal using decision-based coupled window median filter. SIViP. doi:10.1007/s11760-013-0487-5
2. Boudjelaba K, Ros F, Chikouche D (2011) An advanced genetic algorithm for designing 2-D FIR filters. In: 2011 I.E. Pacific Rim Conference on Communications, Computers and Signal Processing, pp 60–65
3. Das S, Abraham A, Konar A (2008) Particle swarm optimization and differential evolution algorithms: technical analysis, applications and hybridization perspectives. Stud Computat Intell (SCI) 116:1–38
4. Das S, Suganthan PN (2011) Differential evolution: a survey of the state-of-the-art. IEEE Trans Evol Comput 15(1):4–31
5. Esakkirajan S, Veerakumar T, Subramanyam AN, PremChand CH (2011) Removal of high density salt and pepper noise through modified decision based unsymmetric trimmed median filter. IEEE Signal Process Lett 18(5):287–290
6. Estrada F, Fleet D, Jepson A (2009) Stochastic image denoising. In: British Machine Vision Conference http://www.cs.utoronto.ca/~strider/Denoise/. Accessed 20 Nov 2011
7. Gonzalez RC, Woods RE (2008) Digital image processing. Prentice Hall, Englewood Cliffs
8. Hua J, Kuang W, Gao Z, Meng L, Xu Z (2012) Image denoising using 2-D FIR filters designed with DEPSO. Multimedia Tools Appl. doi:10.1007/s11042-012-1263-1
9. Huang HC, Chu SC, Pan JS, Huang CY, Liao BY (2011) Tabu search based multi-watermarks embedding algorithm with multiple description coding. Inf Sci 181(16):3379–3396
10. Huang HC, Pan JS, Huang YH, Wang FH, Huang KC (2007) Progressive watermarking techniques using genetic algorithms. Circ Syst Signal Process 26(5):671–687
11. Latif A (2013) An adaptive digital image watermarking scheme using fuzzy logic and tabu search. J Inf Hiding Multimedia Signal Process 4(4):250–271
12. Lim JS (1990) Two dimensional signal and image processing. Prentice Hall, NJ
13. Liu J-C, Tai Y-L (2011) Design of 2-D wideband circularly symmetric FIR filters by multiplierless high-order transformation. IEEE Trans Circ Syst 58(4):746–754
14. McClellan JH, Chan DSK (1977) A 2-D FIR filter structure derived from the Chebyshev recursion. IEEE Trans Circ Syst CAS-24:372–378
15. Srinivasan KS, Ebenezer D (2007) A new fast and efficient decision-based algorithm for removal of high-density impulse noises. IEEE Signal Process Lett 14(4):189–192
16. Sriranganathan S, Bull DR, Redmill DW (1995) Design of 2-D multiplierless FIR filters using genetic algorithms. In: International Conference on Genetic Algorithms in Engineering Systems: Innovations and Applications, pp 282–286
17. Storn R, Price K (1995) Differential evolution: a simple and efficient adaptive scheme for global optimization over continuous spaces. Int Comput Sci Inst, Berkeley: TR-095-012
18. Storn R, Price K (1997) Differential evolution- a simple and efficient heuristic for global optimization over continuous spaces. J Glob Optim 11(4):341–359
19. Thamvichai R, Bose T, Haupt RL (2001) Design of 2-D multiplierless filters using the genetic algorithm. In: Thirty-Fifth Asilomar Conference on Signals, Systems and Computers, 588–591
20. Thamvichai R, Bose T, Haupt RL (2002) Design of 2-D multiplierless IIR filter using the genetic algorithm. IEEE Trans Circ Syst-I Fundam Theory Appl 49(6):878–882
21. Tomasi C, Manduchi R (1998) Bilateral filtering for gray and color images. In: International Conference on Computer Vision, pp 839–846
22. Tzeng S-T (2007) Design of 2-D multiplierless FIR digital filters with specified magnitude and group delay responses by GA approach. Signal Process 87:2036–2044
23. Wang Z, Bovik AC (2004) A universal image quality index. IEEE Signal Process Lett 9(3):81–84
24. Wang Z, Bovik AC, Sheikh HR, Simoncelli EP (2004) Image quality assessment: from error visibility to structural similarity. IEEE Trans Image Process 13(4):600–612
25. Yin H, Qiao J, Fu P, Xia X (2014) Face feature selection with binary particle swarm optimization and support vector machine. J Inf Hiding Multimedia Signal Process 5(4)

Abhijit Chandra received his B.E. in Electronics & Telecommunication Engineering in 2008 from Bengal Engineering & Science University, Shibpur, Howrah-711 103, India and M.E.Tel.E with specialization in Communication Engineering in 2010 from Jadavpur University, Kolkata-700 032, India. He is currently associated with the Department of Instrumentation & Electronics Engineering, Jadavpur University, Kolkata as an Assistant Professor. He has published more than 30 papers in International/National Conferences and Journals of good repute. His research area includes Digital Signal/Image Processing, Evolutionary Optimization Techniques, Digital/Mobile Communication Systems, Information and Coding Theory. He has also been working as a guest reviewer of many internationally acclaimed journals. Mr. Chandra has received President's Gold Medal from Bengal Engineering & Science University, Shibpur in 2010 for being First in the faculty of Engineering and Technology at B.E. examination 2008. He has also received University Medal in 2010 for standing First in order of merit at the M.E. Tel. E. examination 2010 from Jadavpur University.

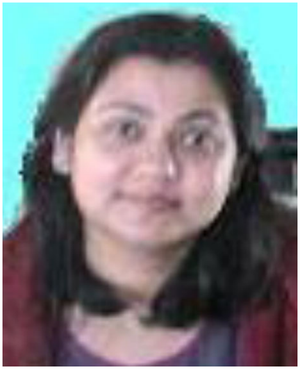

Sudipta Chattopadhyay received her B. Tech degree in Instrumentation Engineering in 1994 from Calcutta University, Kolkata- 700 009, India, and M.E.Tel.E and PhD degrees from Jadavpur University, Kolkata—700 032, India in 2001 and 2012 respectively. She was a Lecturer in the Department of Electronics and Communication Engineering at Institute of Technical Education and Research, Bhubaneswar, India, from 1996 to 2001 and also worked as Lecturer, Sr. Lecturer and Assistant Professor in the Department of Electronics and Communication Engineering at Netaji Subash Engineering College, Kolkata—700 152, India, from 2001 to 2006. She is now working as an Assistant Professor in the Department of Electronics and Telecommunication Engineering, Jadavpur University, Kolkata—700 032, India since 2006. She has published a number of papers in International Conferences and International Journals of repute. Her current research interests include Digital/Mobile Communication, Coding Theory and Digital Signal Processing and Evolutionary Algorithms. Dr. Chattopadhyay is a member of IEEE since last 12 years. She is also an Executive Committee member of the Affinity Group "Women in Engineering" under IEEE Calcutta Section.